

# Highly efficient entanglement swapping for long-distance quantum communication

Rui-Bo Jin

*Researcher*

*National Institute of Information and Communications Technology (NICT), Tokyo, Japan*

**4th international conference on quantum cryptography (Qcrypt2014)**  
Telecom ParisTech, Paris, France 20140905(Fri)

# Highly efficient entanglement swapping for long-distance quantum communication

Rui-Bo Jin<sup>1</sup>, Masahiro Takeoka<sup>1</sup>, Utako Takagi<sup>1,2</sup>, Ryosuke Shimizu<sup>3</sup>, Masahide Sasaki<sup>1</sup>

<sup>1</sup>*National Institute of Information and Communications Technology (NICT), Tokyo, Japan*

<sup>2</sup>*Tokyo University of Science, Tokyo, Japan*

<sup>3</sup>*University of Electro-Communication (UEC), Tokyo, Japan*

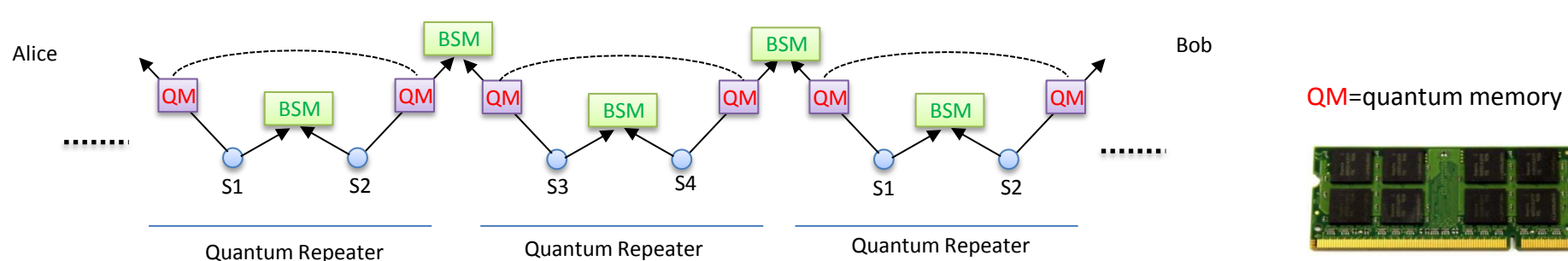
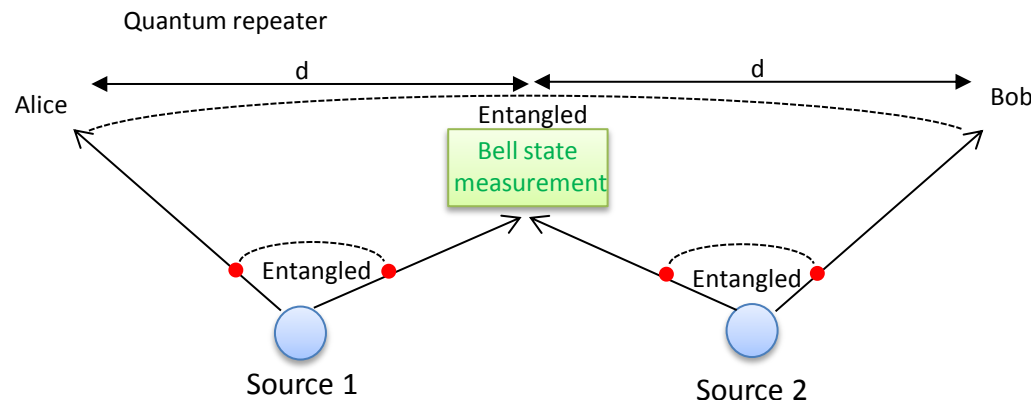
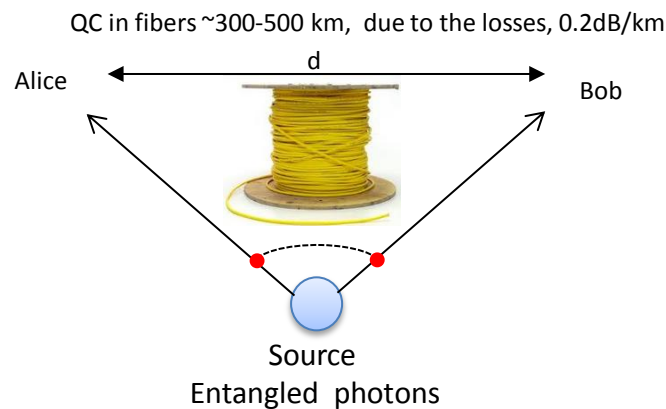
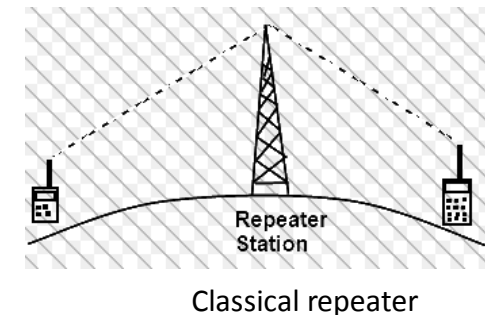
- 1. Motivation**
- 2. Introduction** (entangled sources; SNSPD detectors)
- 3. Experiment**
- 4. Result** (4-fold HOM interference; teleportation; swapping)
- 5. Discussion**
- 6. Conclusion**

# 1. Motivation

## The scenario of quantum repeaters

Global quantum communication requires quantum repeaters

Quantum repeaters need entanglement swapping



Global quantum communication network

Rev. Mod. Phys. **83**, 33(2011)  
Nature **453**, 1023(2008)



## 2. Introduction (1)

### Previous work on entanglement swapping

1. The first entanglement swapping experiment was demonstrated at ~800nm

Pan, et al, PRL. 80, 3891(1998)

2. The previous entanglement swapping experiments at telecom wavelengths

Ref	Material	Wavelength	4-fold coincidence	visibility	application
1. Marcikic2003	LBO	1310nm	0.05cps	70%	teleportation
2. Riedmatten2005	LBO	1310nm	0.004cps	80%	swapping
3. Halder2007	PPLN-WG	1560nm	0.0003cps	77%	swapping
4. Takesue2009	fiber	1551nm	0.038cps	64%	swapping
5. Xue2012	DSF (fiber)	1550nm	0.016cps	75%	swapping
6. Wu2013	PPLN WG	1550nm	0.08cps	92%	swapping

**The low count rates :**

long accumulation time to obtain reliable data → big obstacle for quantum communication.

**Two reasons :** low-efficiency entangled sources + low-efficiency detectors.

## 2. Introduction (2)

### Photon sources from PPKTP crystal

In type II SPDC in PPKTP crystal, the group velocities are matched around 1584nm

$$V_g^{-1}(\omega_s) + V_g^{-1}(\omega_i) = V_g^{-1}(\omega_p)$$

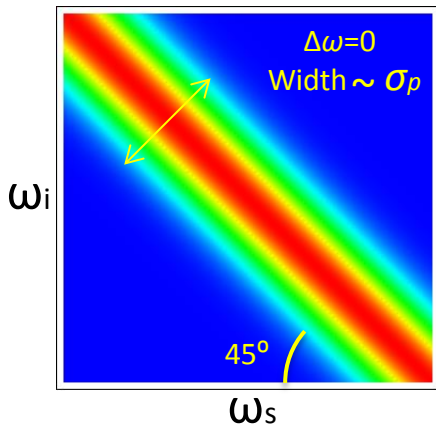


GVM condition:

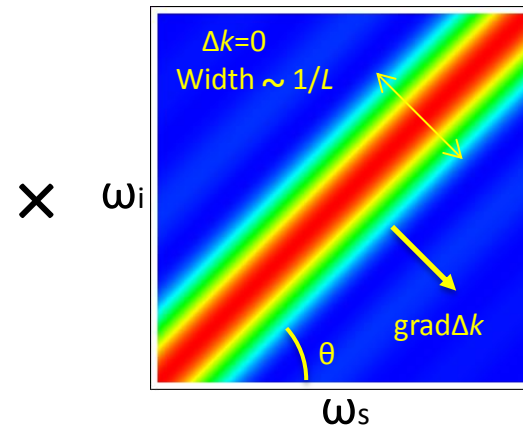
Grice, et al, PRA 56, 1627 (1997).  
Konig, et al, APL 84, 1644 (2004).  
Eckstein, et al, PRL 106, 013603 (2011).

Jin, et al, Opt. Express 21, 10659 (2013)

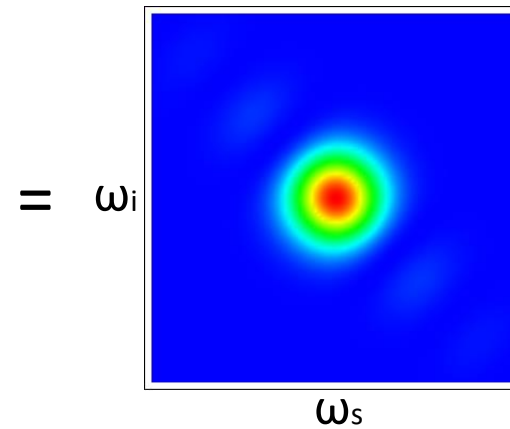
(a) Pump envelop intensity



(b) Phase matching intensity



(c) Joint spectral intensity



$$|\alpha(\omega_s, \omega_i)|^2 = \exp\left[-\left(\frac{\omega_s + \omega_i - \omega_p}{\sigma}\right)^2\right]$$

$$|\phi(\omega_s, \omega_i)|^2 = (\text{Sinc}[\frac{\Delta k L}{2}])^2$$

$$|f(\omega_s, \omega_i)|^2 = |\alpha(\omega_s, \omega_i)|^2 |\phi(\omega_s, \omega_i)|^2$$

Group velocity matched → High spectral purity → no need for narrow band pass filters<sup>5</sup>

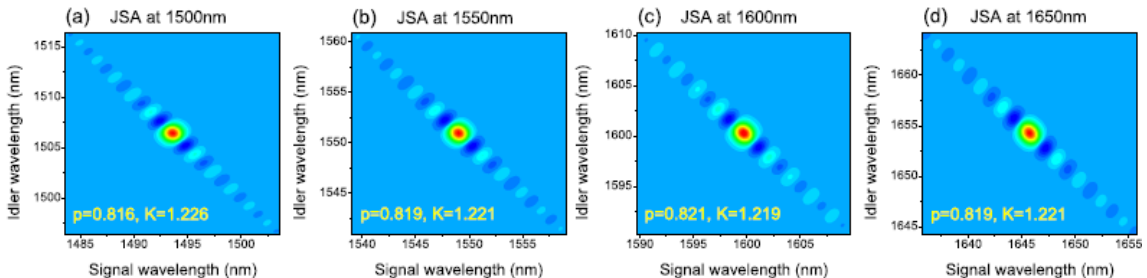
## 2. Introduction (3)

### GVM-PPKTP photon source

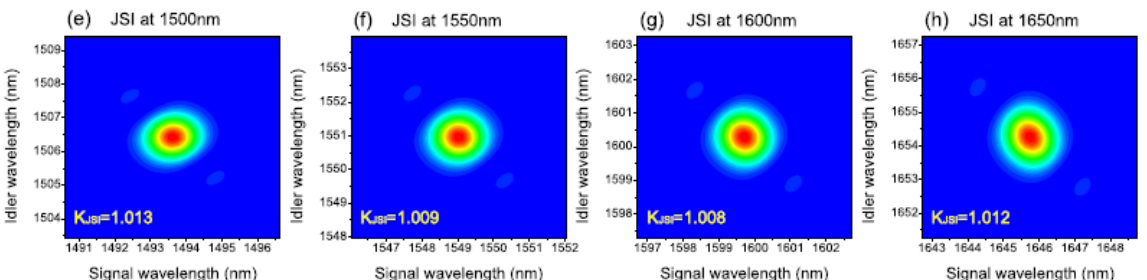
High spectral purity and wide tunability

#### Simulation data

Joint  
spectral  
amplitude

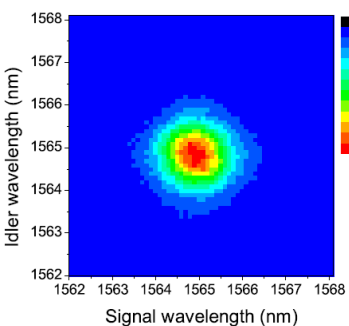


Joint  
spectral  
intensity

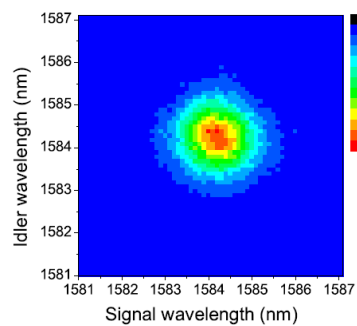


#### Experimentally measured data

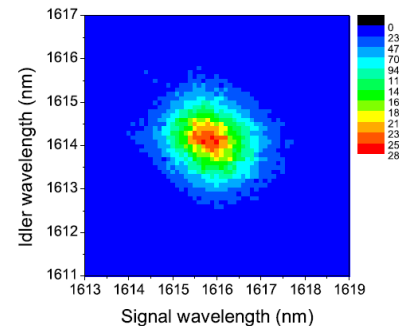
(a)  $K_{JSI}=1.011$ , at 1565 nm



(b)  $K_{JSI}=1.017$ , at 1584 nm



(c)  $K_{JSI}=1.044$ , at 1615 nm

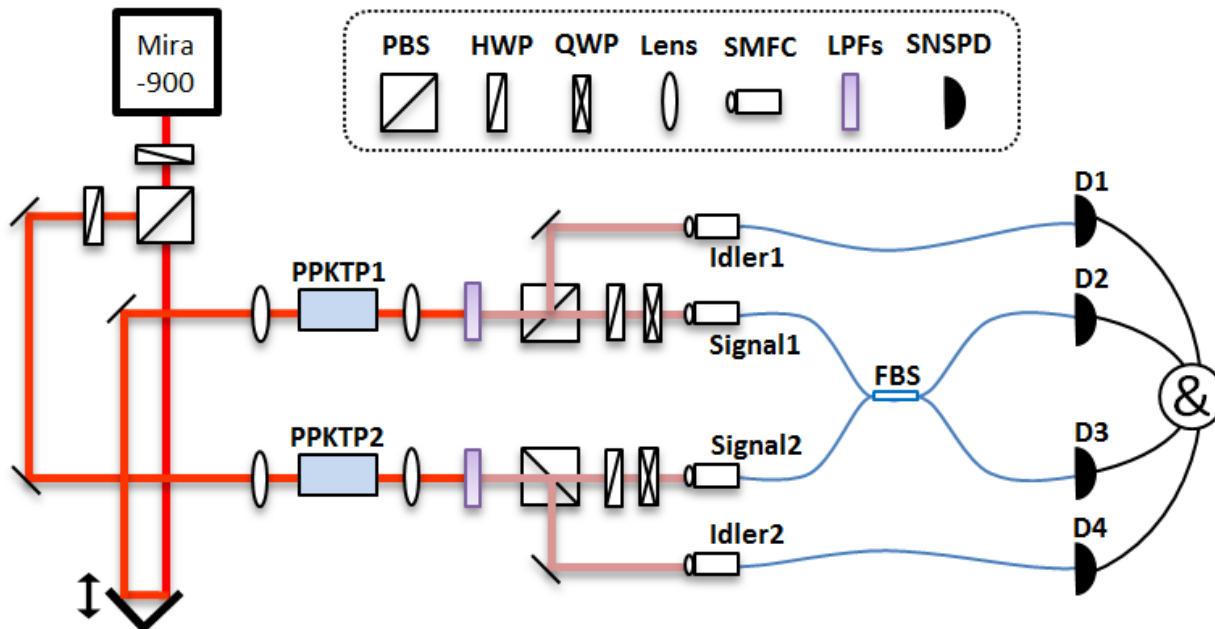


Jin, et al, Opt. Express 21, 10659 (2013)

## 2. Introduction (4)

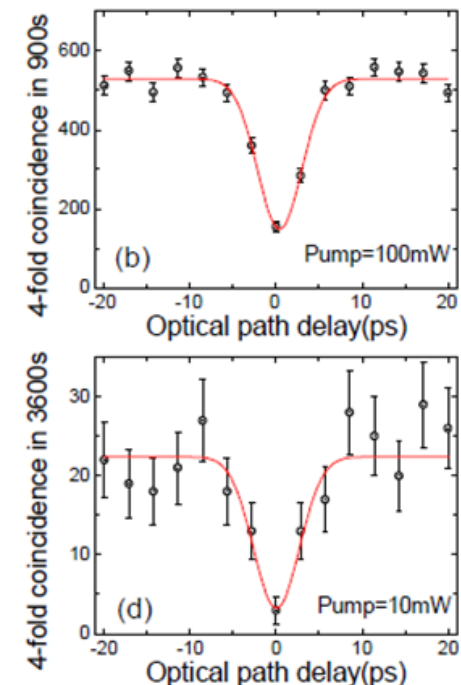
Spectral purity is important for multi-photon interference

Jin, et al, PRA 87, 063801 (2013)



High visibility of 85.5+8% was achieved without using any BPF.  
Because the intrinsic spectral purity is high.

4-fold HOM interference



Hong-Ou-Mandel interference

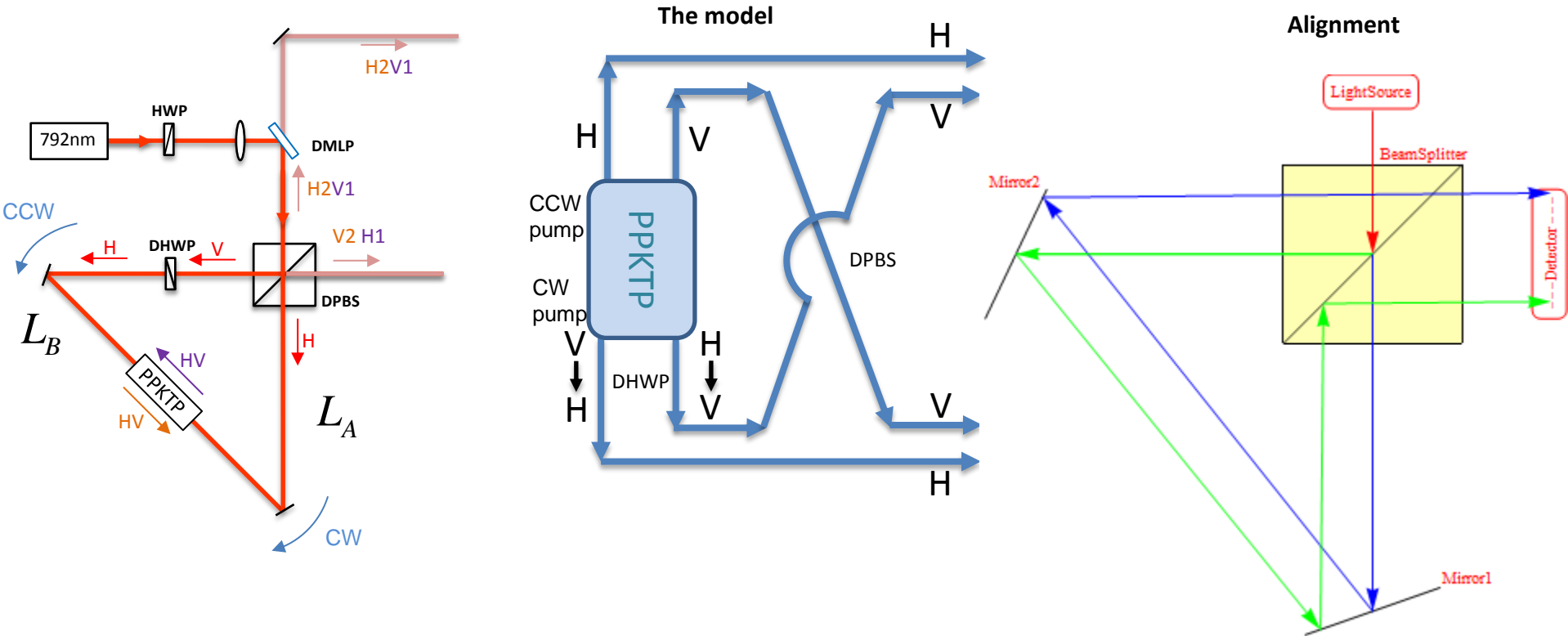
Hong et al, PRL 59, 2044 (1987)

## 2. Introduction (5)

From single photon source to entangled photon source

### Sagnac-GVM-PPKTP entangled source

Sagnac interferometer → Highly stable; no temporal walk-off



Kim, et al, PRA 73, 012316 (2006)

Wong, et al, Laser Physics 16, 1517(2006)

Jin, et al, Opt. Express 22, 11498 (2014)

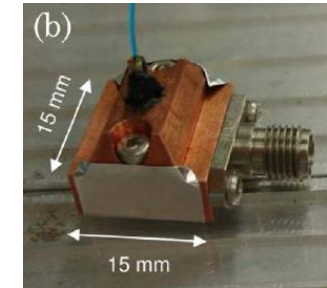
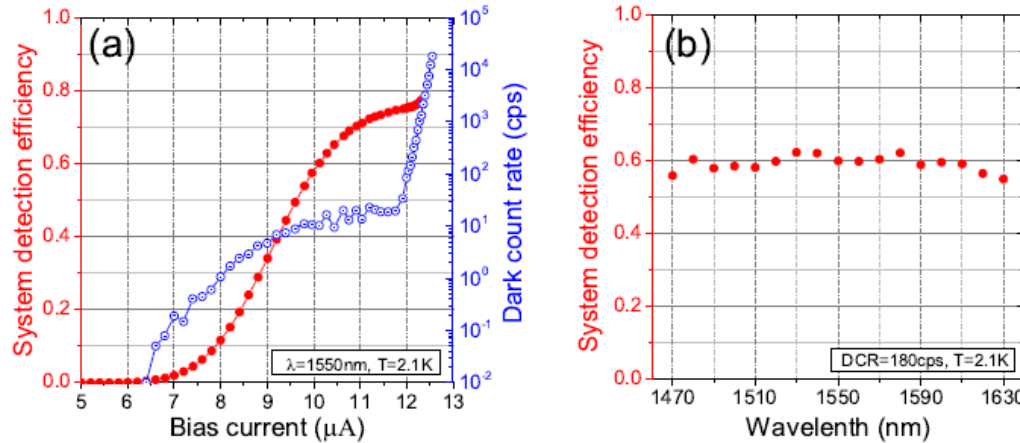
Takeoka, et al, will submit soon (2014)

<http://demonstrations.wolfram.com/SagnacInterferometer/> (open source)  
<https://www.youtube.com/watch?v=Ju-Ca3iT5ns>

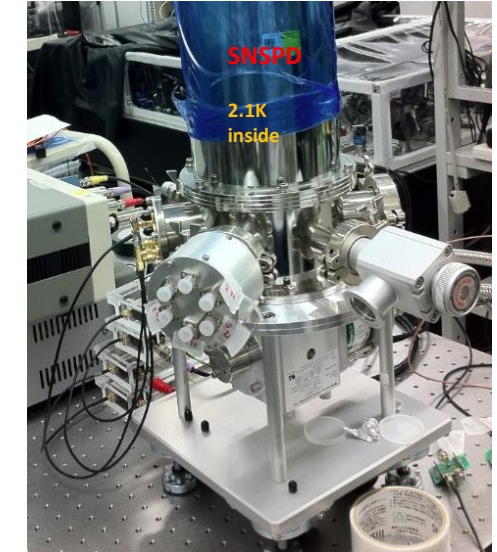
## 2. Introduction (6)

We have good detectors: Superconducting nanowire single photon detectors (SNSPD)

High efficiency: detecting efficiency > 70% dark counts ~ 1 kcps  
recovery time = 40 ns, time jitter = 68 ps  
spectral range: 1470-1630nm



Miki, *et al*, Opt. Express 21, 10208 (2013)  
Yamashita, *et al*, Opt. Express 21, 27177 (2013)  
Miki, *et al*, IEEE Trans. Appl. Sc. 17, 285 (2007)



Test with single photon source

Single counts=5.23Mcps

Coincidence=1.17Mcps

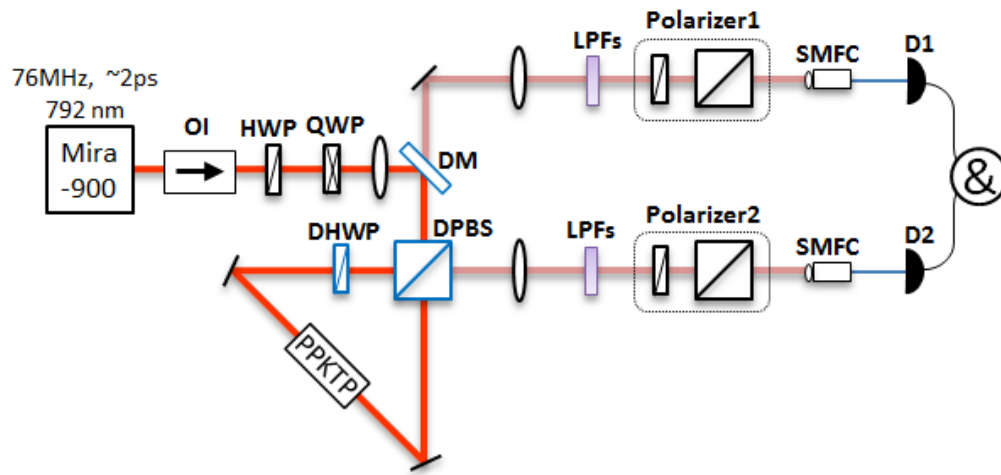
at 400mW pump

the highest ever reported at telecom wavelengths

## 2. Introduction (7)

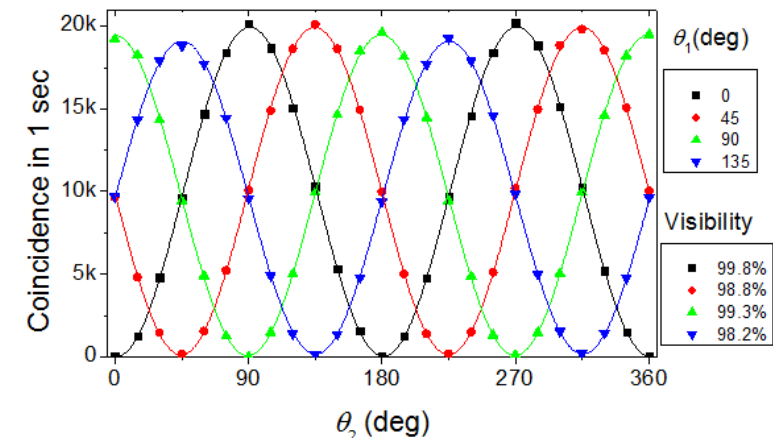
### Performance of our entangled source

Jin, et al, Opt. Express 22, 11498 (2014)



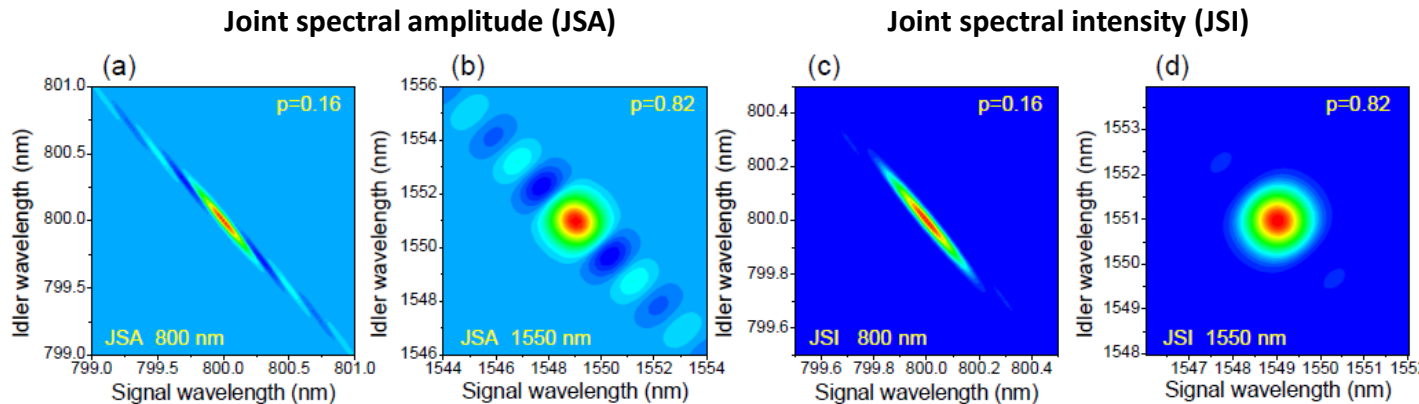
Beam waist= 45  $\mu\text{m}$   
PPKTP=30mm, type II  
@1584nm

SNSPD efficiency=0.7  
Coupling efficiency= 0.5  
Overall efficiency=0.2



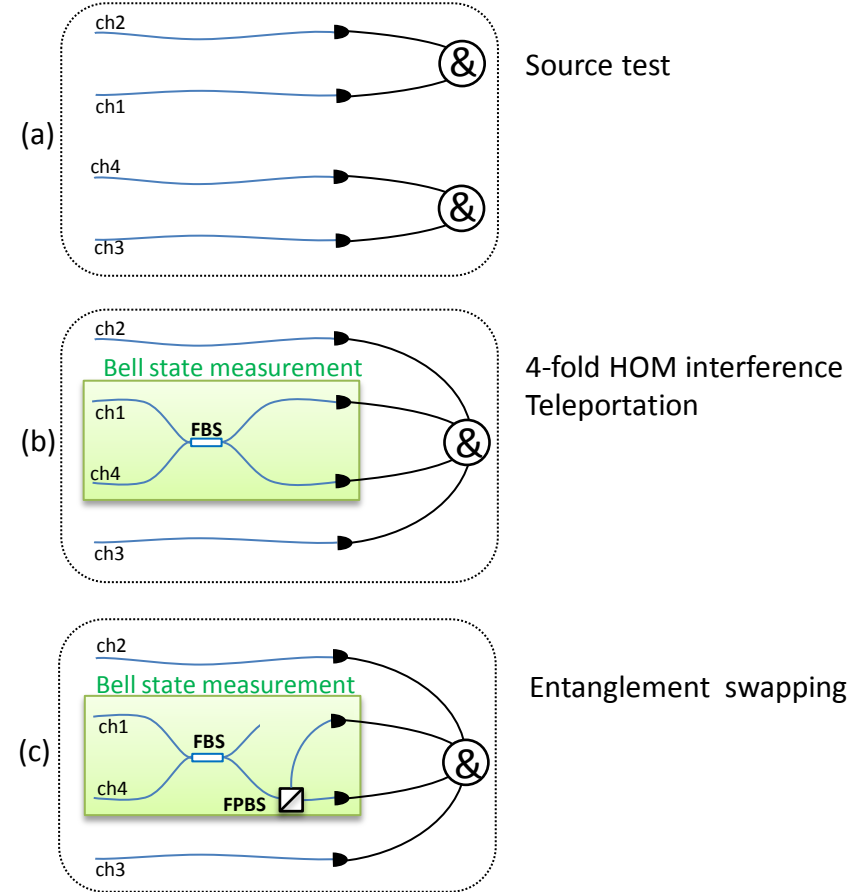
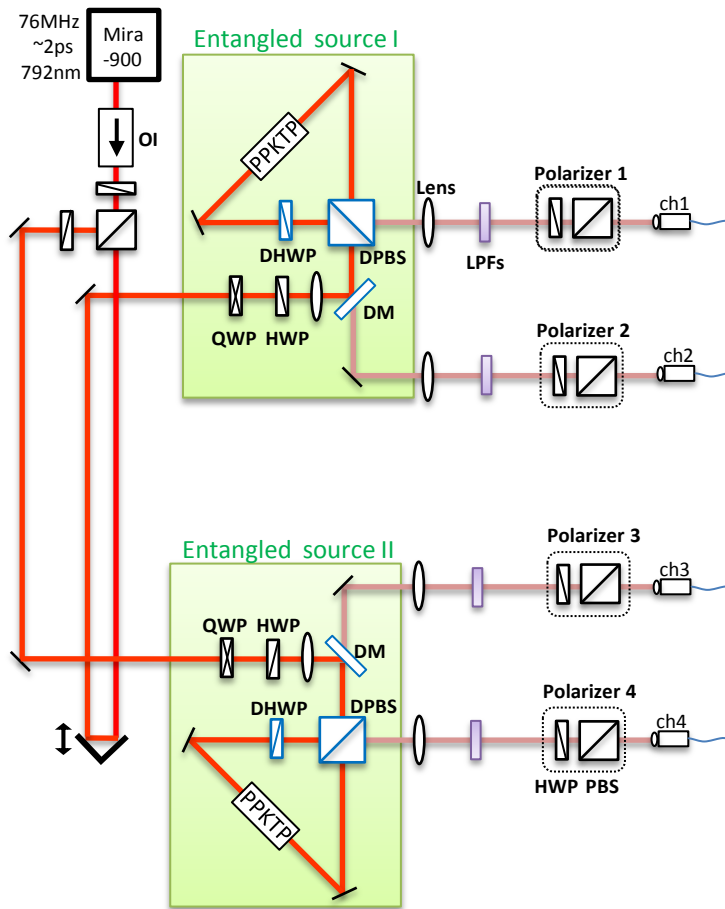
Coincidence=40 kcps @ 10mW  
Visibility>98% for all bases  
Spectral purity=0.82

Advantages of our entangled source: Stable; intrinsically high purity; telecom wavelength



### 3. Experiment (1)

#### Experimental setup

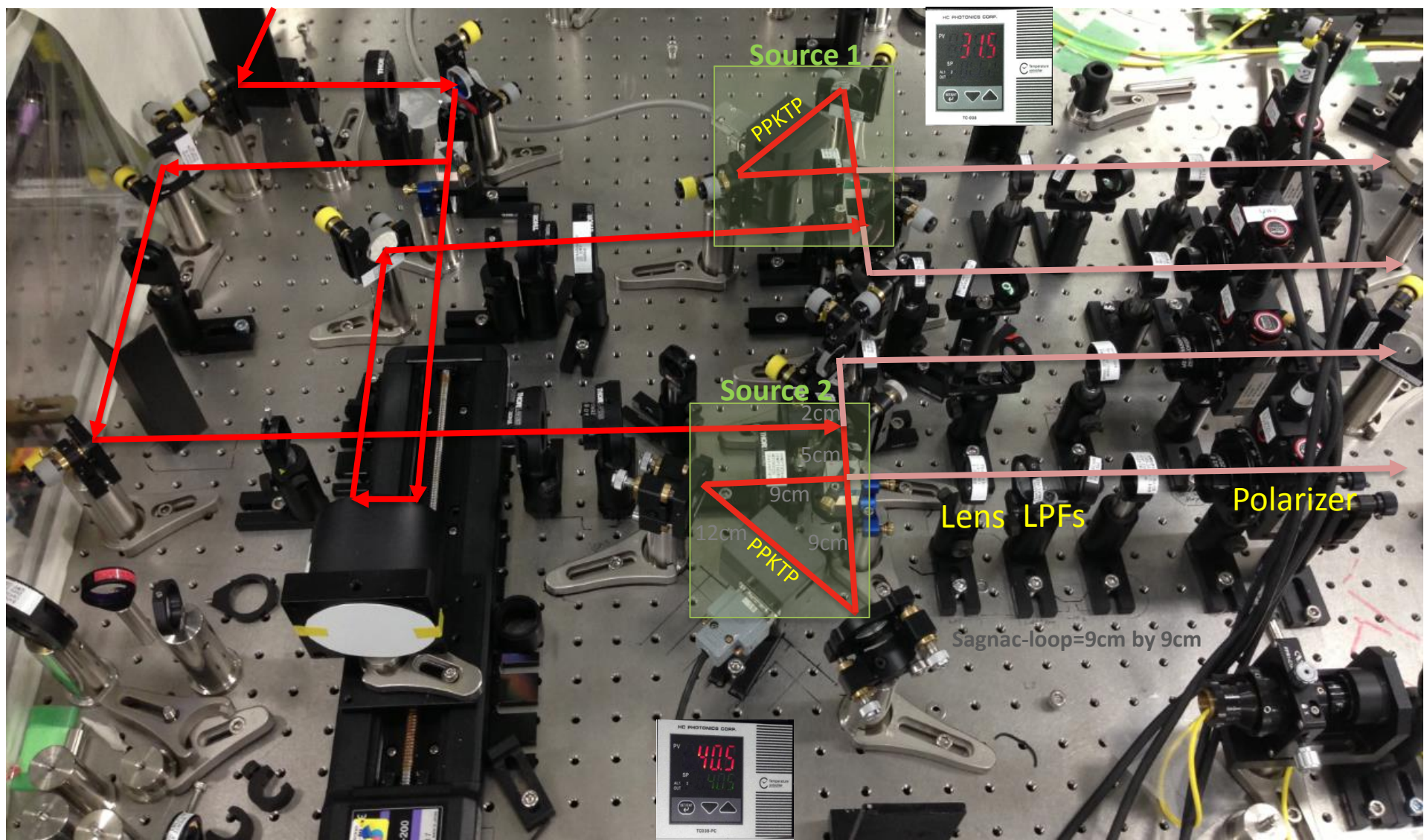


PPKTP: 30-mm-long , poling period =  $46.1\ \mu\text{m}$ ,  
type-II group-velocity-matched SPDC, degenerate.  
The temperature for PPKTP=31.0/40.5 °C

80mW—Source I      85mW—Source II  
Average photon numbers per pulse ~0.1

### 3. Experiment (2)

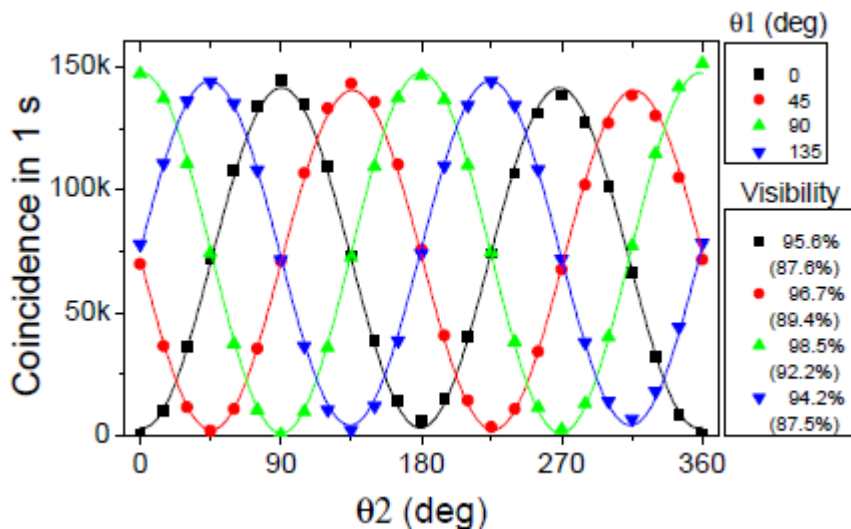
#### Experimental setup



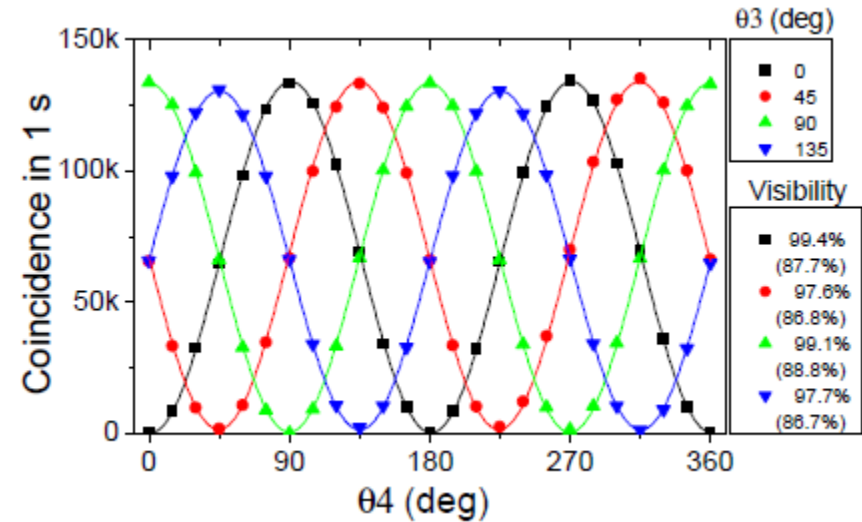
# 4. Result (1)

## Polarization correlation measurement (EPR interference)

(a) Source I  $|\psi^-\rangle$



(b) Source II  $|\psi^-\rangle$



Pump: 80/85mW, accumulate in 1 sec, coincidence counts~150 kcps  
 net V~97%, raw V~87%, Average photon numbers per pulse~0.1

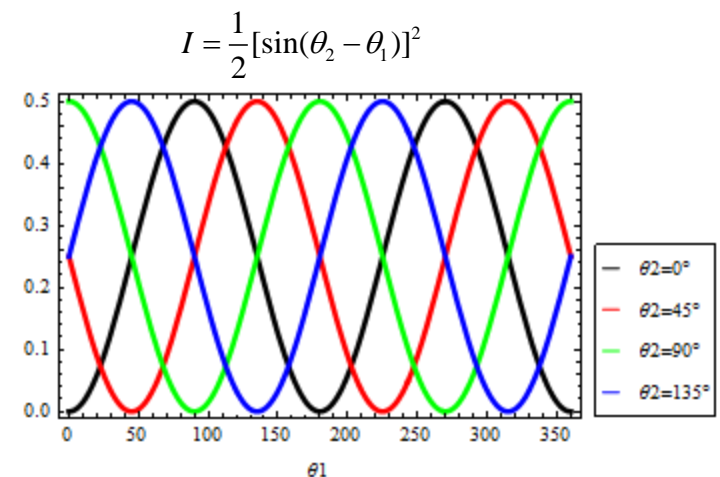
Net visibility  
 (Raw visibility)

### Theory calculation

$$|\psi^-\rangle = \frac{1}{\sqrt{2}}(|H_1V_2\rangle - |V_1H_2\rangle) \quad I = \frac{1}{2}[\sin(\theta_2 - \theta_1)]^2$$

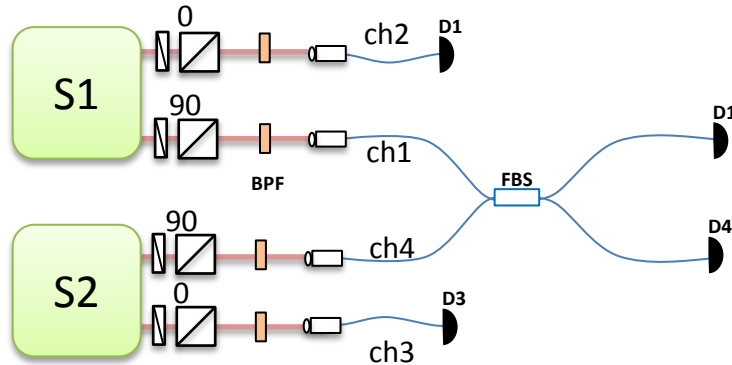
$$|\theta_1\rangle = \cos \theta_1 |H_1\rangle + \sin \theta_1 |V_1\rangle \quad (\text{with } HWP_1 = \theta_1/2), \quad |\theta_2\rangle = \cos \theta_2 |H_2\rangle + \sin \theta_2 |V_2\rangle$$

$$\langle \theta_2 | \langle \theta_1 | \psi^-\rangle = \frac{1}{\sqrt{2}}[\sin \theta_2 \cos \theta_1 - \cos \theta_2 \sin \theta_1] = \frac{1}{\sqrt{2}} \sin(\theta_2 - \theta_1)$$

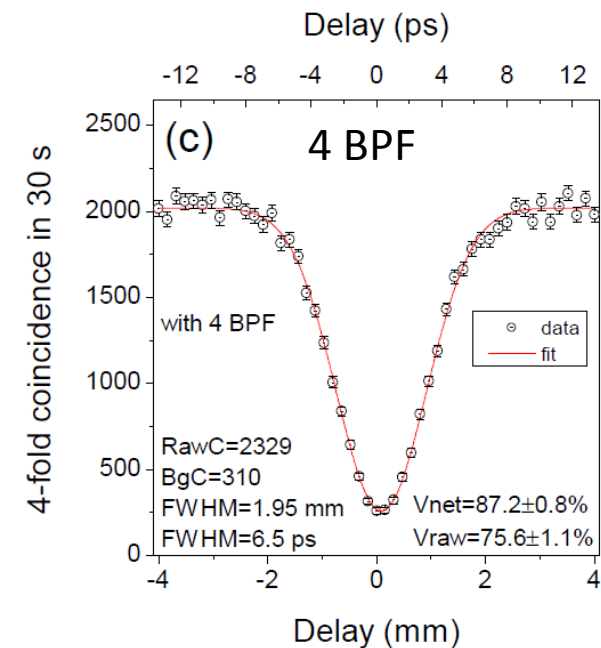
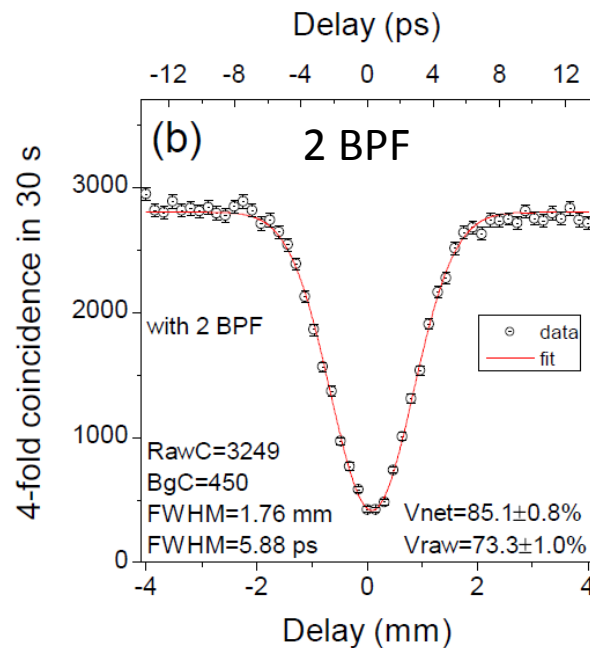
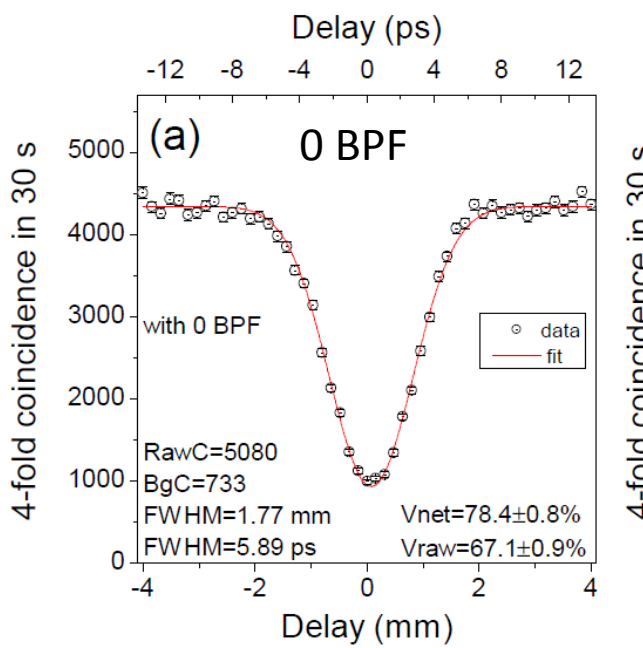


# 4. Result (2)

## 4-fold Hong-Ou-Mandel (HOM) interference

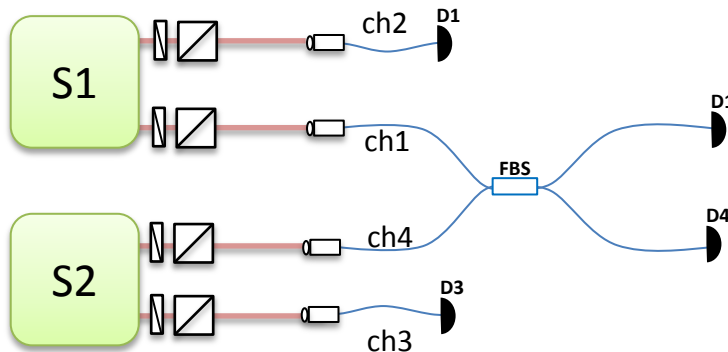


Number	No BPF	2BPF	4BPFs
Raw visibility	67.1%	73.3%	75.6%
Net visibility	78.4%	85.1%	87.2%
4-fold coincidence	169cps	108cps	78cps
background	24cps	15cps	10cps

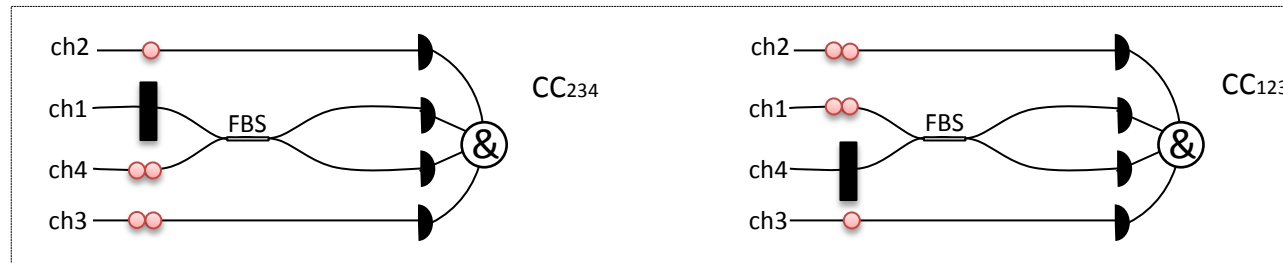


# 4. Result (3)

## How to subtract background in 4-fold HOM interference



Number	No BPF	2BPF	4BPFs
Raw visibility	67.1%	73.3%	75.6%
Net visibility	78.4%	85.1%	87.2%
4-fold coincidence	169cps	108cps	78cps
background	24cps	15cps	10cps



Background counts= CC<sub>234</sub>+CC<sub>123</sub>

Contributed by multi-photon emission

Soller, et al, PRA 83, 031806 (2011)  
Jin , et al, PRA 87, 063801 (2013)

# 4. Result (4)

Visibility is determined by spectral purity

$$V = \text{Tr}[\rho_1 \rho_2] = \frac{\text{Tr}[\rho_1^2] + \text{Tr}[\rho_2^2] - \|\rho_1 - \rho_2\|^2}{2}$$

Purity of source1, source 2

Indistinguishability of source1 and 2

visibility

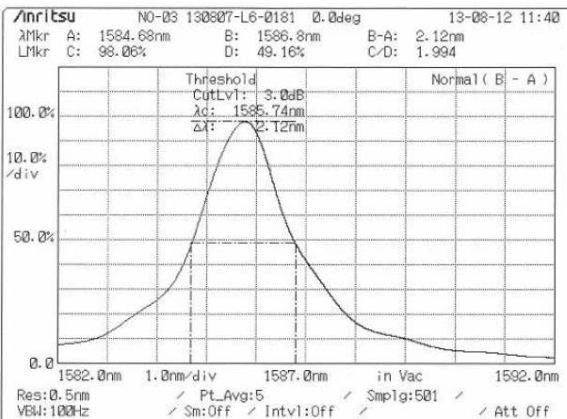
Jin, et. al, PRA 87, 063801 (2013)

Osorio, et. al, J Phys. B 46, 055501 (2013).

Mosley et. al, PRL 100, 133601 (2008).

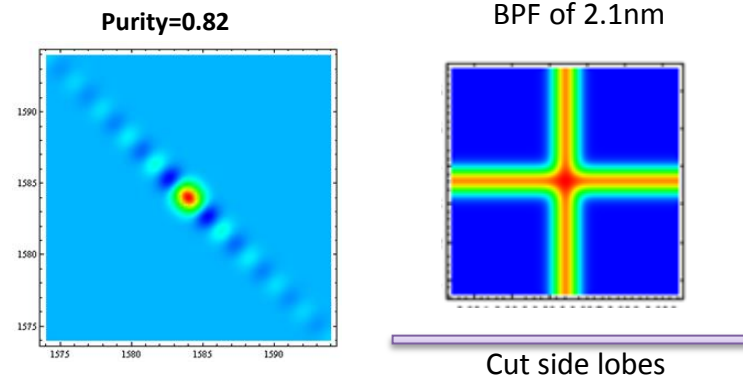
Lee, et. al, PRL 91 087902(2003)

Coarse BPF



FWHM of the BPF=2.1nm  
FWHM of the source=1.1nm  
FWHM after filter=1.0nm

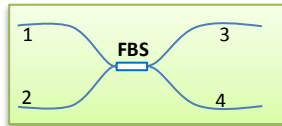
With small loss we can improve the purity from 0.82 to 0.99



# 4. Result (5) Teleportation: Bell state measurement-1

Bell state analyzer  
Rev. Mod. Phys. **84**, 777(2012)

If the input state is



BS :

$$\hat{a}_1 = (\hat{a}_3 + \hat{a}_4)/\sqrt{2}$$

$$\hat{a}_2 = (\hat{a}_3 - \hat{a}_4)/\sqrt{2}$$

$$|\psi^-\rangle = \frac{1}{\sqrt{2}}(|H_1V_2\rangle - |V_1H_2\rangle)$$

$$H_1 = \frac{1}{\sqrt{2}}(H_3 + H_4) \quad H_2 = \frac{1}{\sqrt{2}}(H_3 - H_4) \quad V_1 = \frac{1}{\sqrt{2}}(V_3 + V_4) \quad V_2 = \frac{1}{\sqrt{2}}(V_3 - V_4)$$

$$H_1V_2 = \frac{1}{2}(H_3 + H_4)(V_3 - V_4) = \frac{1}{2}(H_3V_3 - H_4V_4 - H_3V_4 + H_4V_3)$$

$$V_1H_2 = \frac{1}{2}(V_3 + V_4)(H_3 - H_4) = \frac{1}{2}(H_3V_3 - H_4V_4 + H_3V_4 - H_4V_3)$$

$$H_1V_2 - V_1H_2 = H_4V_3 - H_3V_4 \quad H_1V_2 + V_1H_2 = H_3V_3 - H_4V_4$$

$$|\psi^-\rangle = \frac{1}{\sqrt{2}}(|H_1V_2\rangle - |V_1H_2\rangle) \xrightarrow{BS} \frac{1}{\sqrt{2}}(|H_3V_4\rangle - |V_3H_4\rangle)$$

$$|\psi^+\rangle = \frac{1}{\sqrt{2}}(|H_1V_2\rangle + |V_1H_2\rangle) \xrightarrow{BS} \frac{1}{\sqrt{2}}(|H_3V_3\rangle - |V_3H_4\rangle)$$

$$|\phi^+\rangle = \frac{1}{\sqrt{2}}(|H_1H_2\rangle + |V_1V_2\rangle) \xrightarrow{BS} \frac{1}{2}[|H_3H_3\rangle - |H_4H_4\rangle + (|V_3V_3\rangle - |V_4V_4\rangle)]$$

$$|\phi^-\rangle = \frac{1}{\sqrt{2}}(|H_1H_2\rangle - |V_1V_2\rangle) \xrightarrow{BS} \frac{1}{2}[|H_3H_3\rangle - |H_4H_4\rangle - (|V_3V_3\rangle - |V_4V_4\rangle)]$$

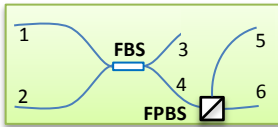
Conclusion: only when  $|\psi^-\rangle$  state inputs, CC exists.  
So, a CC means the  $|\psi^-\rangle$  state is detected

Partial Bell state measurement

# 4. Result (6)

## Teleportation: Bell state measurement-2

Bell state analyzer  
Rev. Mod. Phys. 84,777(2012)



If the input state is

*PBS :*

$$\hat{a}_{4H} = \hat{a}_{6H} \quad \hat{a}_{4V} = \hat{a}_{5V}$$

*BS + PBS :*

$$\hat{a}_{1H} = (\hat{a}_{3H} + \hat{a}_{4H})/\sqrt{2} = \hat{a}_{6H}/\sqrt{2}$$

$$\hat{a}_{1V} = (\hat{a}_{3V} + \hat{a}_{4V})/\sqrt{2} = \hat{a}_{5V}/\sqrt{2}$$

$$\hat{a}_{2H} = (\hat{a}_{3H} - \hat{a}_{4H})/\sqrt{2} = -\hat{a}_{6H}/\sqrt{2}$$

$$\hat{a}_{2V} = (\hat{a}_{3V} - \hat{a}_{4V})/\sqrt{2} = -\hat{a}_{5V}/\sqrt{2}$$

$$|\psi^-\rangle = \frac{1}{\sqrt{2}}(|H_1V_2\rangle - |V_1H_2\rangle) \xrightarrow{BS} \frac{1}{\sqrt{2}}(|H_3V_4\rangle - |V_3H_4\rangle) \quad \text{There is no CC at port 5/6}$$

$$|\psi^+\rangle = \frac{1}{\sqrt{2}}(|H_1V_2\rangle + |V_1H_2\rangle) \xrightarrow{BS} \frac{1}{\sqrt{2}}(|H_3V_3\rangle - |V_4H_4\rangle) \quad \text{There is CC at port 5/6}$$

$$|\phi^+\rangle = \frac{1}{\sqrt{2}}(|H_1H_2\rangle + |V_1V_2\rangle) \xrightarrow{BS} \frac{1}{2}[(|H_3H_3\rangle - |H_4H_4\rangle) + (|V_3V_3\rangle - |V_4V_4\rangle)]$$

$$|\phi^-\rangle = \frac{1}{\sqrt{2}}(|H_1H_2\rangle - |V_1V_2\rangle) \xrightarrow{BS} \frac{1}{2}[(|H_3H_3\rangle - |H_4H_4\rangle) - (|V_3V_3\rangle - |V_4V_4\rangle)]$$

There is no CC at port 5/6

Conclusion: A CC detection means the  $|\psi^+\rangle$  state is detected

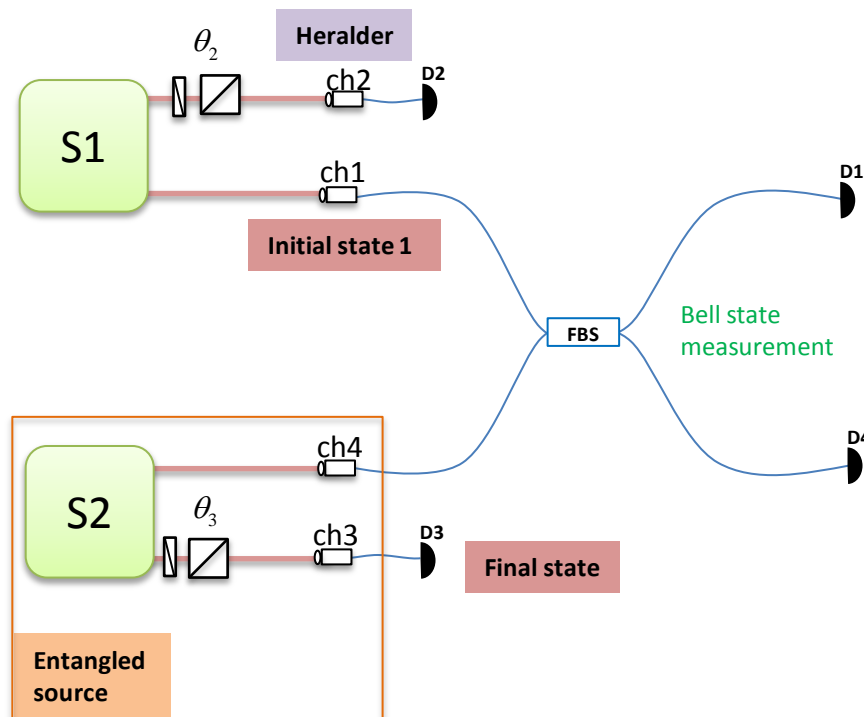
# 4. Result (7)

## The principle of teleportation

$$|\psi^-\rangle_{34} \otimes |i\rangle_1 = \frac{1}{\sqrt{2}} (\langle HV| - \langle VH|)_{34} \underbrace{(\alpha|H\rangle + \beta|V\rangle)_1}_{}$$

$$\equiv \frac{1}{2} [\langle \psi^+ \rangle_{41} (-\alpha|H\rangle + \beta|V\rangle)_3 + \underbrace{\langle \psi^- \rangle_{41} (\alpha|H\rangle + \beta|V\rangle)_3}_{\text{ }} + \langle \phi^+ \rangle_{41} (\alpha|V\rangle - \beta|H\rangle)_3 + \langle \phi^- \rangle_{41} (\alpha|V\rangle + \beta|H\rangle)_3]$$

$$|\psi^-\rangle_{34} \otimes (\alpha|H\rangle_1 + \beta|V\rangle_1) \xrightarrow{BSM} \frac{1}{2} |\psi^-\rangle_{14} (\alpha|H\rangle_3 + \beta|V\rangle_3)$$



$ch_1 \xrightarrow{\text{teleport}} ch_3$

e.g. 1

$$\begin{aligned} Ch2 : (|V\rangle) &\xrightarrow{\text{Herald}} Ch1 : (|H\rangle) \xrightarrow{\text{BSM select}} Ch3 : (|H\rangle) \\ \Rightarrow Ch3 = 0^\circ &\rightarrow CC \text{ exist} \rightarrow \text{no HOM dip } (\theta_2 / \theta_3 = 90^\circ / 0^\circ) \\ Ch3 = 90^\circ &\rightarrow \text{no CC} \rightarrow \text{HOM dip } (\theta_2 / \theta_3 = 90^\circ / 90^\circ) \end{aligned}$$

e.g. 2

$$\begin{aligned} Ch2 : (|H\rangle + |V\rangle) &\xrightarrow{\text{Herald}} Ch1 : (|H\rangle - |V\rangle) \xrightarrow{\text{BSM select}} Ch3 : (|H\rangle - |V\rangle) \\ \Rightarrow Ch3 = 45^\circ &\rightarrow \text{CC} \rightarrow \text{HOM dip } (\theta_2 / \theta_3 = 45^\circ / 45^\circ) \\ Ch3 = 135^\circ &\rightarrow \text{CC} \rightarrow \text{HOM dip } (\theta_2 / \theta_3 = 45^\circ / 135^\circ) \end{aligned}$$

# 4. Result (8)

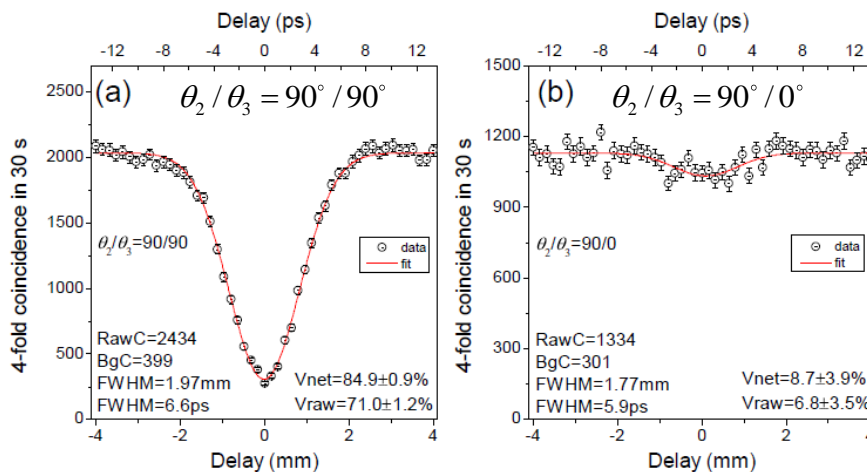
## Teleportation Result

e.g. 1

$Ch2:(|V\rangle) \xrightarrow{\text{Herald}} Ch1:(|H\rangle) \xrightarrow{\text{BSM select}} Ch3:(|H\rangle)$

$\Rightarrow Ch3=0^\circ \rightarrow CC \text{ exist} \rightarrow \text{no HOM dip } (\theta_2 / \theta_3 = 90^\circ / 0^\circ)$

$Ch3=90^\circ \rightarrow \text{no CC} \rightarrow \text{HOM dip } (\theta_2 / \theta_3 = 90^\circ / 90^\circ)$

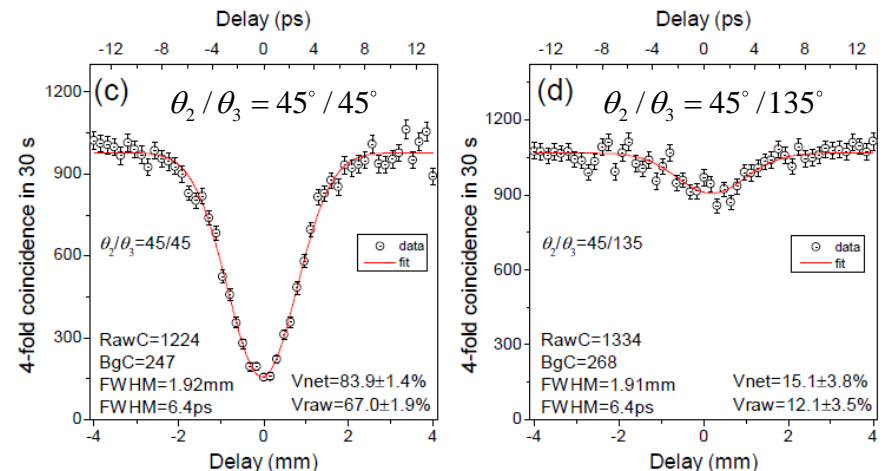


e.g. 2

$Ch2:(|H\rangle+|V\rangle) \xrightarrow{\text{Herald}} Ch1:(|H\rangle-|V\rangle) \xrightarrow{\text{BSM select}} Ch3:(|H\rangle-|V\rangle)$

$\Rightarrow Ch3=45^\circ \rightarrow \text{no CC} \rightarrow \text{HOM dip } (\theta_2 / \theta_3 = 45^\circ / 45^\circ)$

$Ch3=135^\circ \rightarrow \text{CC} \rightarrow \text{no HOM dip dip } (\theta_2 / \theta_3 = 45^\circ / 135^\circ)$

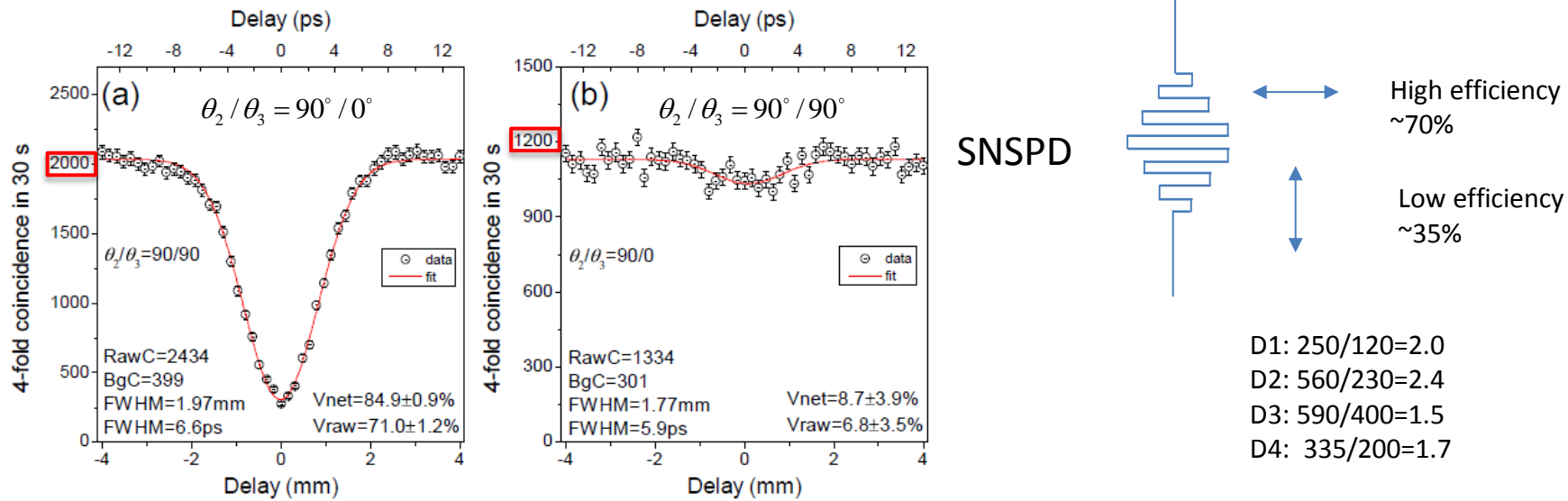


## Teleportation at other angles

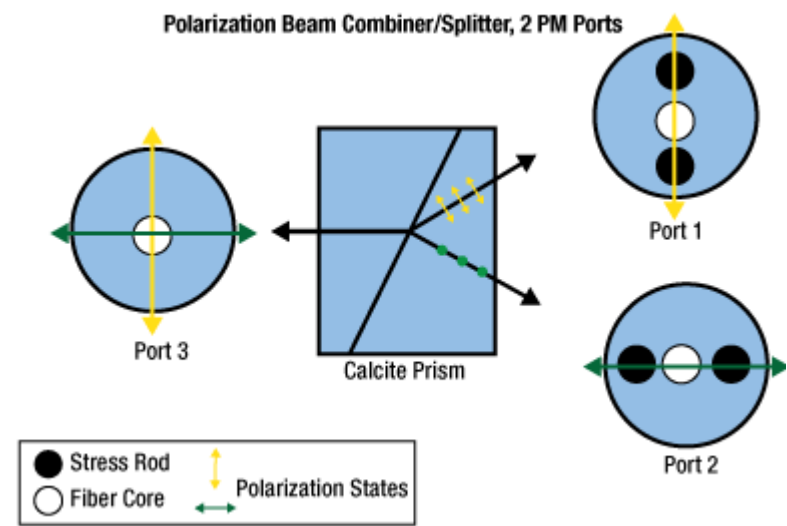
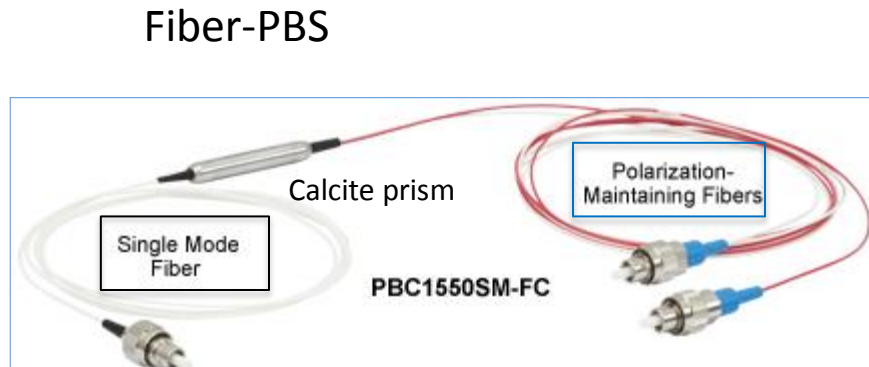
$\theta_2 / \theta_3$	Raw Visibility	Net Visibility	Ideal		$\theta_2 / \theta_3$	Raw Visibility	Net Visibility	Ideal
0/0	56%	75.8%	100%		45/45	66.9%	83.9%	100%
0/90	11.4%	14.2%	0%		45/135	12.0%	15.1%	0%
90/0	6.8%	8.7%	0%		135/45	13.2%	16.9%	0%
90/90	71%	84.9%	100%		135/135	65.9%	81.9%	100%

# 4. Result (9)

## Polarization dependency of SNSPD's efficiency



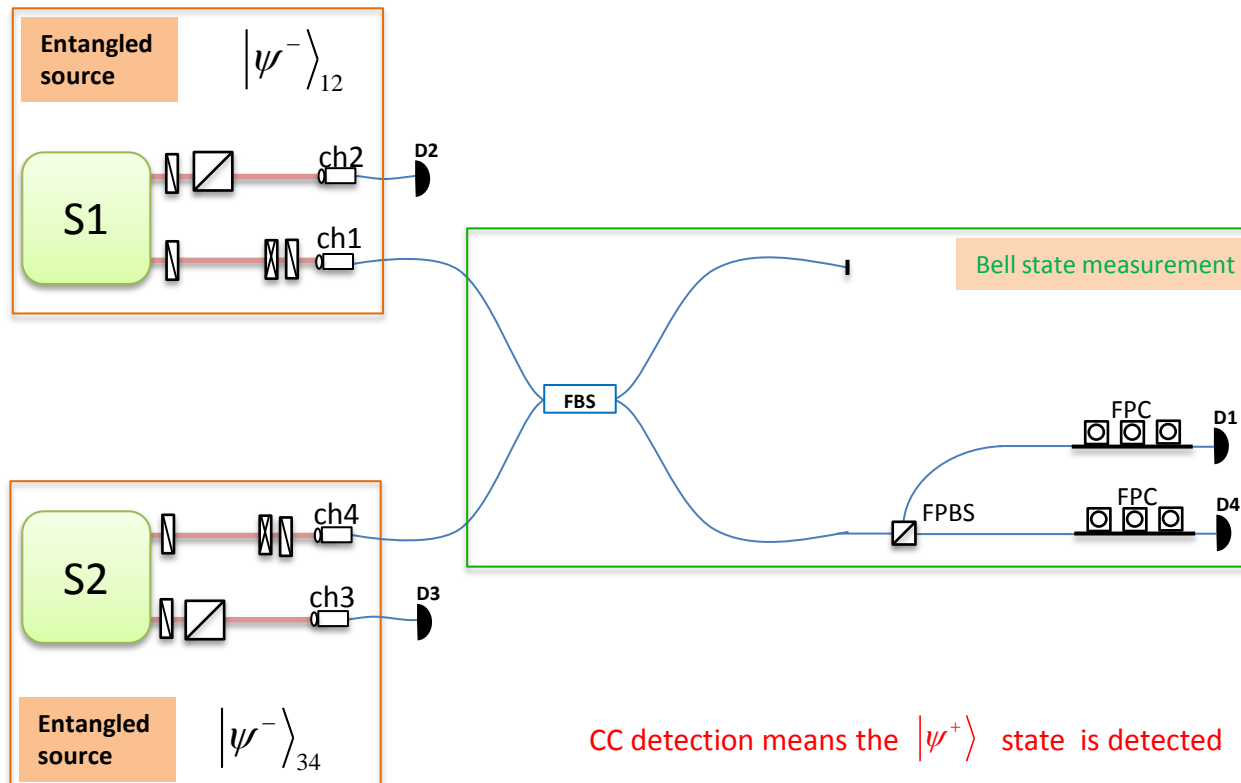
How to overcome this problem?



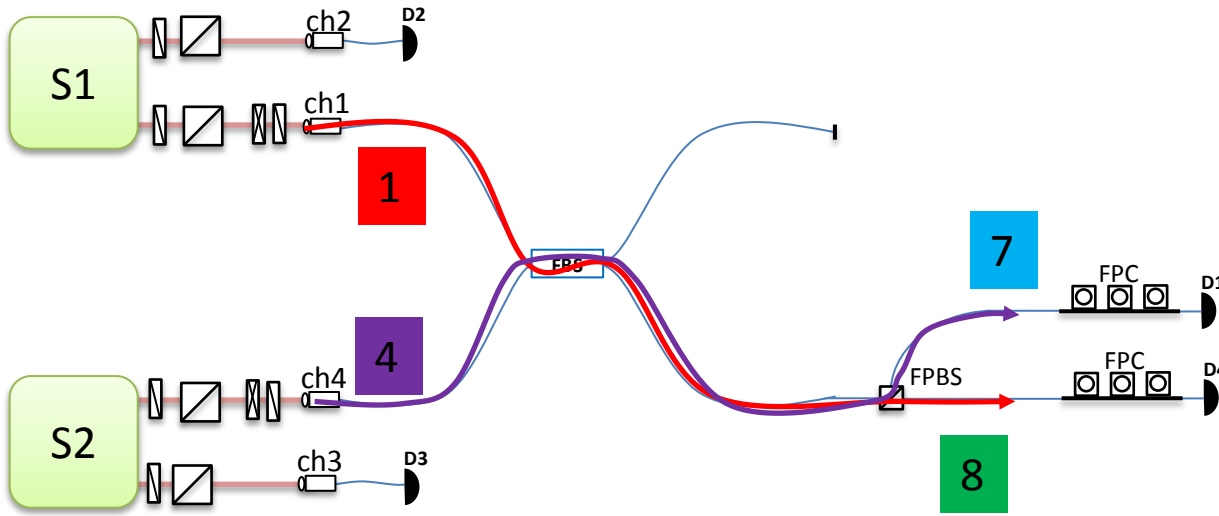
## 4. Result (10) The principle of entanglement swapping

$$|\psi^-\rangle_{12} \otimes |\psi^-\rangle_{34} \equiv \frac{1}{2} (|\psi^+\rangle_{14} \otimes |\psi^+\rangle_{23} - |\psi^-\rangle_{14} \otimes |\psi^-\rangle_{23} - |\phi^+\rangle_{14} \otimes |\phi^+\rangle_{23} + |\phi^-\rangle_{14} \otimes |\phi^-\rangle_{23})$$

$$|\psi^-\rangle_{12} \otimes |\psi^-\rangle_{34} \xrightarrow{BSM} |\psi^+\rangle_{14} \otimes |\psi^+\rangle_{23}$$



# 4. Result (11) Entanglement swapping Calibration



$$H_1 \rightarrow 8 \quad H_4 \rightarrow 7$$



$$H_1 \xrightarrow{HWPQWP} H_1$$

$$H_4 \xrightarrow{HWPQWP} V_4$$



$$\left| \psi^{\pm} \right\rangle_{14} \xleftarrow{HWPQWP} \left| \phi^{\pm} \right\rangle_{14}$$

$$\left| \psi^- \right\rangle_{12} \otimes \left| \psi^- \right\rangle_{34} \equiv \frac{1}{2} (\left| \psi^+ \right\rangle_{14} \otimes \left| \psi^+ \right\rangle_{23} - \left| \psi^- \right\rangle_{14} \otimes \left| \psi^- \right\rangle_{23} - \left| \phi^+ \right\rangle_{14} \otimes \left| \phi^+ \right\rangle_{23} + \left| \phi^- \right\rangle_{14} \otimes \left| \phi^- \right\rangle_{23})$$

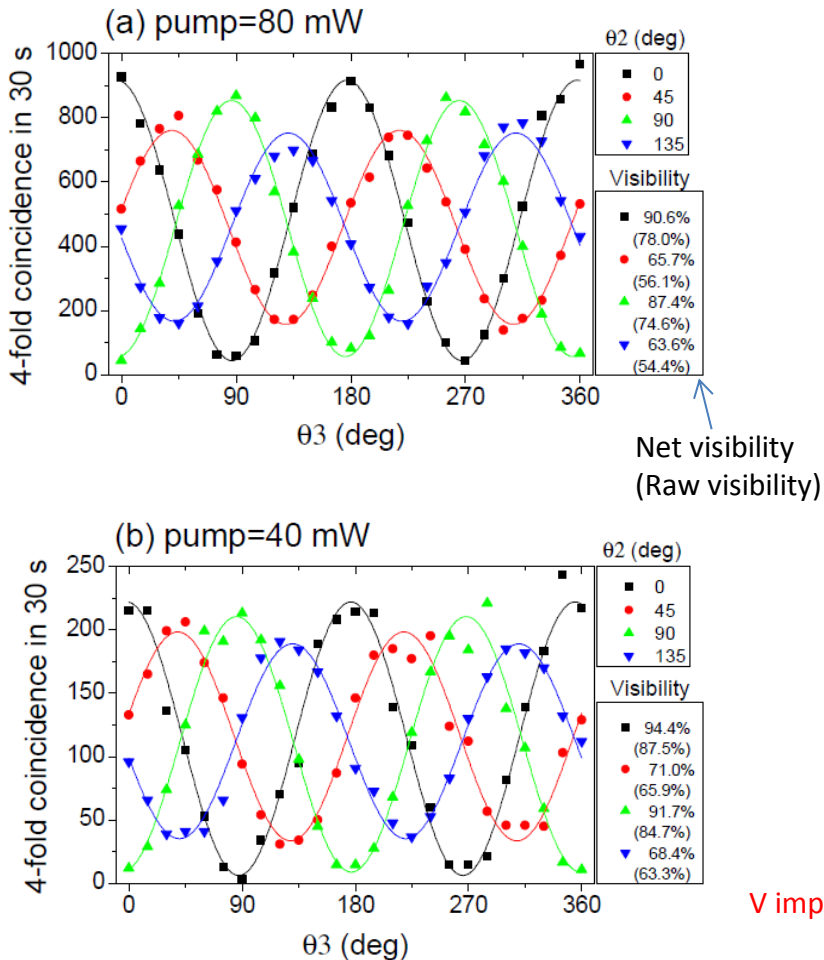


$$\left| \psi^- \right\rangle_{12} \otimes \left| \psi^- \right\rangle_{34} \rightarrow \frac{1}{2} (\underbrace{\left| \phi^+ \right\rangle_{14} \otimes \left| \psi^+ \right\rangle_{23} - \left| \phi^- \right\rangle_{14} \otimes \left| \psi^- \right\rangle_{23}}_{\left| \psi^+ \right\rangle_{14} \otimes \left| \phi^+ \right\rangle_{23}} + \left| \psi^- \right\rangle_{14} \otimes \left| \phi^- \right\rangle_{23})$$

## 4. Result (12) Entanglement swapping

$$\left| \psi^- \right\rangle_{12} \otimes \left| \psi^- \right\rangle_{34} \rightarrow \frac{1}{2} (\left| \phi^+ \right\rangle_{14} \otimes \left| \psi^+ \right\rangle_{23} - \left| \phi^- \right\rangle_{14} \otimes \left| \psi^- \right\rangle_{23} - \left| \psi^+ \right\rangle_{14} \otimes \left| \phi^+ \right\rangle_{23} + \left| \psi^- \right\rangle_{14} \otimes \left| \phi^- \right\rangle_{23})$$

$$\left| \psi^- \right\rangle_{12} \otimes \left| \psi^- \right\rangle_{34} \xrightarrow{HWPQWP+BSM} \left| \psi^+ \right\rangle_{14} \otimes \left| \phi^+ \right\rangle_{23}$$



### Theory calculation

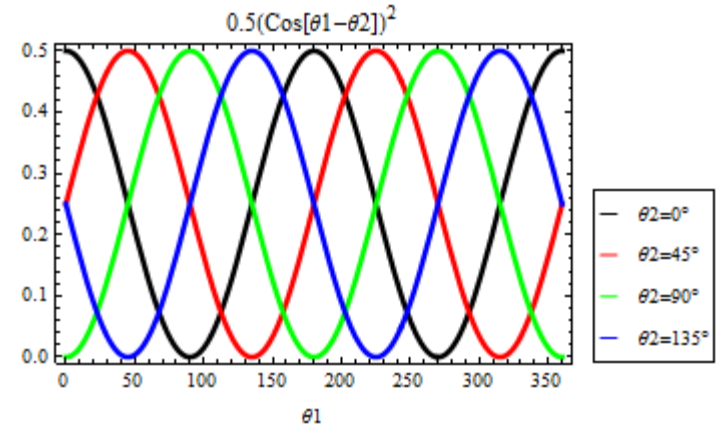
$$\left| \phi^+ \right\rangle = \frac{1}{\sqrt{2}} (\left| H_1 H_2 \right\rangle + \left| V_1 V_2 \right\rangle)$$

$$\left| \theta_1 \right\rangle = \cos \theta_1 \left| H_1 \right\rangle + \sin \theta_1 \left| V_1 \right\rangle \quad (\text{with } HWP_1 = \theta_1 / 2),$$

$$\left| \theta_2 \right\rangle = \cos \theta_2 \left| H_2 \right\rangle + \sin \theta_2 \left| V_2 \right\rangle$$

$$\langle \theta_2 | \langle \theta_1 | \psi^- \rangle = \frac{1}{\sqrt{2}} [\cos \theta_2 \cos \theta_1 + \sin \theta_2 \sin \theta_1] = \frac{1}{\sqrt{2}} \cos(\theta_2 - \theta_1)$$

$$I = \frac{1}{2} [\cos(\theta_2 - \theta_1)]^2$$



V improved by 7%

## 5. Discussion (1) Comparison of the 4-fold coincidence counts

With the previous experiments at ~1550nm

Ref	Material	Wavelength	4-fold coincidence	HOM visibility	application
[1]. Marcikic2003	LBO	1310nm	0.05cps	70%	teleportation
[2]. Riedmatten2005	LBO	1310nm	0.004cps	80%	swapping
[3]. Halder2007	PPLN-WG	1560nm	0.0003cps	77%	swapping
[4]. Takesue2009	fiber	1551nm	0.038cps	64%	swapping
[5]. Xue2012	DSF (fiber)	1550nm	0.016cps	75%	swapping
[6]. Wu2013	PPLN WG	1550nm	0.08cps	92%	swapping
<b>This work</b>	<b>PPKTP</b>	<b>1584nm</b>	<b>108cps</b>	<b>78%</b>	<b>swap./telep.</b>

**Our count rate is 3 orders higher than the previous schemes**

**Highly bright sources + highly efficient detectors**

- [1] Marcikic, *et al*, Nature 421, 509 (2003).
- [2] Riedmatten, *et al*, PRA. 71, 050302 (2005).
- [3] Halder, *et al*, Nat. Phys. 3, 629 (2007).
- [4] Takesue , *et al*, Opt. Express 17, 10748 (2009)
- [5] Xue, *et al*, PRA. 85, 032337(2012)
- [6] Wu , *et al*, J. Phys.B 46, 235503 (2013)

## 5. Discussion (2) Comparison with the best performance at $\sim 800$ nm

Ref	Material	Wavelength	2-fold coincidence	HOM Visibility	application
[1]. Herbst2014	BBO	808nm	$C_2=130$ kcps	60%	Swap. 143km
[2]. Yin2012	BBO	808nm	$C_2=440$ kcps	60%	Telep. 100km
[3]. Yao2012	BBO	780nm	$C_2=310$ kcps	76%	8-photon entangled state
[4]. Huang2011	BBO	780nm	$C_2=220$ kcps	82%	8-photon entangled state
This work	PPKTP	1584nm	$C_2=150$ kcps	78%(raw)	Swap./Telep.

### Future application

- Free space test of teleportation/swapping at telecom wavelengths
- 6,8,10-photon entangled state generation at telecom wavelengths

The brightness of the source is ready.

The efficiency of the SNSPD is ready.

[1] Herbst, *et al*, arXiv:1403.0009.

[2] Yin, *et al*, Nature 488, 185 (2012).

[3] Yao, *et al*, Nat. Photon. 6, 225 (2012).

[4] Huang , *et al*, Nat. Commun. 2, 546 (2011).

## 5. Discussion (3)

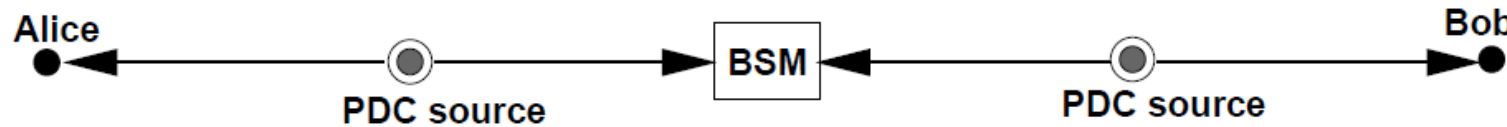
### Application for the future quantum repeater

Global quantum communication network with quantum repeaters



## 5. Discussion (4)

### Application for entanglement swapping based QKD



Ref: Artur Scherer, *et al*, Opt. Express **19**, 3004 (2011).

To demonstrate ES-QKD

Lowest requirement:

1. Four-fold coincidence count rate  $> 10\text{cps}$
2. All visibility  $> 71\%$  to violate the Bell Inequality

Compare with decoy-state-QKD

Advantage: Long distance

Disadvantage: Low count rate

It is scientifically meaningful to demonstrate ES-QKD...

## 5. Discussion (5)

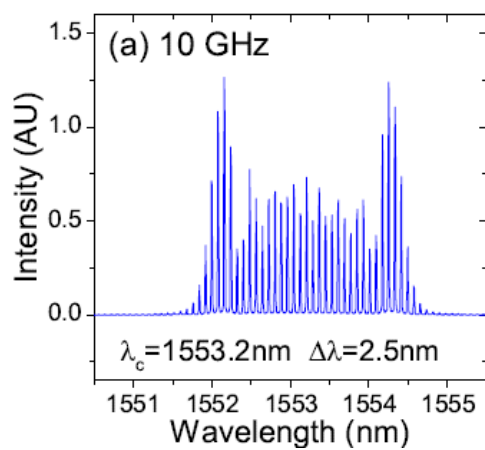
### How to decrease the multi-pair emission

#### Using high repetition rate laser

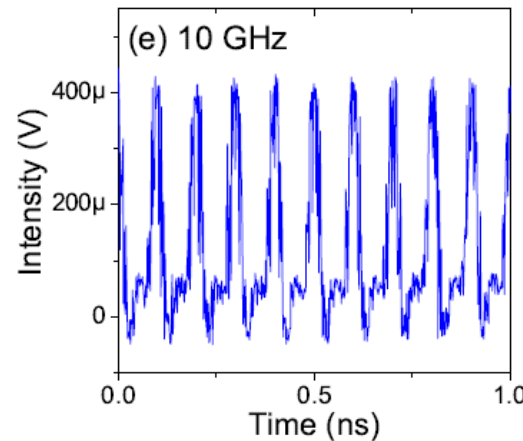
Low average power per pulse → low multi-pair emission  
high repetition rate → high count rate



**Spectrum**



**Time sequence**



**10 GHz repetition-rate comb laser**

Efficient generation of twin photons at telecom wavelengths with 10 GHz repetition-rate-tunable comb laser  
Jin, et al, submitted (2014)

# 6. Conclusion

- ✓ 1. The setup of our entanglement swapping and teleportation experiments

GVM-PPKTP-Sagnac

+

SNSPDs

- ✓ 2. The performance of our entanglement swapping

HOM interference visibility: raw 73%, net 85%

4-fold Coincidence: 108cps

Teleportation visibility: 84.9%

Entanglement swapping visibility: 68.4% to 94.4%

- ✓ 3. Future application

arXiv: 1409.XXXX, will submit soon  
Jin, *et al*, Opt. Express 22, 11498 (2014)  
Jin, *et al*, arXiv: 1309.1221  
Jin, *et al*, Opt. Express 21, 10659 (2013)  
Jin, *et al*, PRA 87, 063801 (2013)

Field test of entanglement swapping/ teleportation

6 photon Entangled state generation at telecom wavelength

Quantum repeater

Entanglement swapping based QKD

Thank you !